Building and Environment 71 (2014) 81–94

Contents lists available at ScienceDirect

Building and Environment

journal homepage: www.elsevier.com/locate/buildenv

# Improving airflow measurement accuracy in VAV terminal units using flow conditioners

Ran Liu [a,b,*], Jin Wen [a], Michael S. Waring [a]

[a] Department of Civil, Architectural and Environmental Engineering, Drexel University, Curtis 251, 3141 Chestnut St., Philadelphia, PA 19104, USA
[b] Iowa Energy Center Energy Resource Station, DMACC Building #23, 2006 S. Ankeny Blvd., Ankeny, IA 50023, USA

ARTICLE INFO

*Article history:*
Received 22 June 2013
Received in revised form
21 September 2013
Accepted 25 September 2013

*Keywords:*
Flow conditioner
VAV
Airflow measurement
Inlet condition
Airflow reading error

ABSTRACT

A variable air volume (VAV) terminal unit adjusts its supply airflow rate to meet the heating or cooling load and/or the ventilation requirement of the served space. Consequently, the accuracy of the VAV airflow sensor is highly important to the VAV system operation, and an inaccuracy of the VAV airflow sensor could lead to an energy waste or insufficient ventilation. ASHRAE Research Project (RP) 1353 identified non-ideal inlet conditions, such as an elbow or kinked duct before the VAV terminal unit, as causes of observed inaccuracies of up to 45% in VAV airflow measurements. VAV airflow measurement errors are normally mitigated by on-site balancing; however, it is difficult to achieve accurate reference airflow measurements in the field because of limited straight ductwork before VAV terminal units, as well as ductwork leakage. This study explored the potential solution of using a VAV flow conditioner to regulate the velocity profile upstream of the VAV airflow sensor and increase the VAV airflow measurement accuracy. A variety of flow conditioners were evaluated with computational fluid dynamics (CFD) modeling, and a CFD-optimized prototype of a 60%-porosity K-Lab/Laws plate was fabricated and tested. For all tested inlet conditions, airflow rates, and VAV boxes, the prototype reduced the VAV airflow reading error to ±5% when it was installed immediately before the VAV box inlet, regardless of upstream duct conditions. The prototype flow conditioner had a pressure drop equivalent to that of a 2-row VAV reheat coil.



## 1. Introduction

### 1.1. Problem statement

Heating, ventilating, and air conditioning (HVAC) systems are the largest energy consumers in modern commercial buildings, using about 30% of building energy [1], so reducing the energy used by the HVAC system is an important goal. Because of their ability to provide better energy efficiency, variable air volume (VAV) systems with direct digital controllers (DDC) have been widely adopted in commercial, industrial, and large residential buildings. A VAV terminal unit adjusts its supply air temperature and airflow rate based on the real time heating and cooling loads, as well as the ventilation requirement, of the space that the system is serving.

Fig. 1 shows a typical configuration of a VAV terminal unit. Typically, there is an airflow sensor at the inlet of a VAV terminal unit that measures the airflow rate passing through the VAV box and that rate is sent as a signal to the VAV controller. The VAV controller compares this measured airflow rate to an airflow set point that is determined based on the heating or cooling and/or ventilation demands. If a significant difference exists, the VAV controller commands the actuator to either open or close the VAV damper position and thus change the airflow to some new amount. Obviously, the accuracy of the VAV airflow sensor is crucial. If the VAV airflow measurement is larger than the true airflow rate, the space ventilation requirement would not be satisfied or the reheating equipment could be damaged [2]; if the VAV airflow measurement is lower than the true airflow rate, then energy would be wasted. Based on standard fan laws, the fan power is proportional to the airflow rate to the third order [2], so, for example, a 40% airflow reading error could result in ~170% fan energy waste. In addition, more heating or cooling energy is consumed to condition the extra airflow.

ASHRAE Research Project (RP) 1353 [3,4] systematically evaluated different VAV terminal units to identify major factors that

* Corresponding author. Present address: Iowa Energy Center Energy Resource Station, DMACC Building #23, 2006 S. Ankeny Blvd., Ankeny, IA 50023, USA. Tel.: +1 515 965 7345; fax: +1 515 965 7056.
*E-mail addresses:* rliu@iastate.edu (R. Liu), jinwen@drexel.edu (J. Wen), msw59@drexel.edu (M.S. Waring).

0360-1323/$ – see front matter © 2013 Elsevier Ltd. All rights reserved.
http://dx.doi.org/10.1016/j.buildenv.2013.09.015

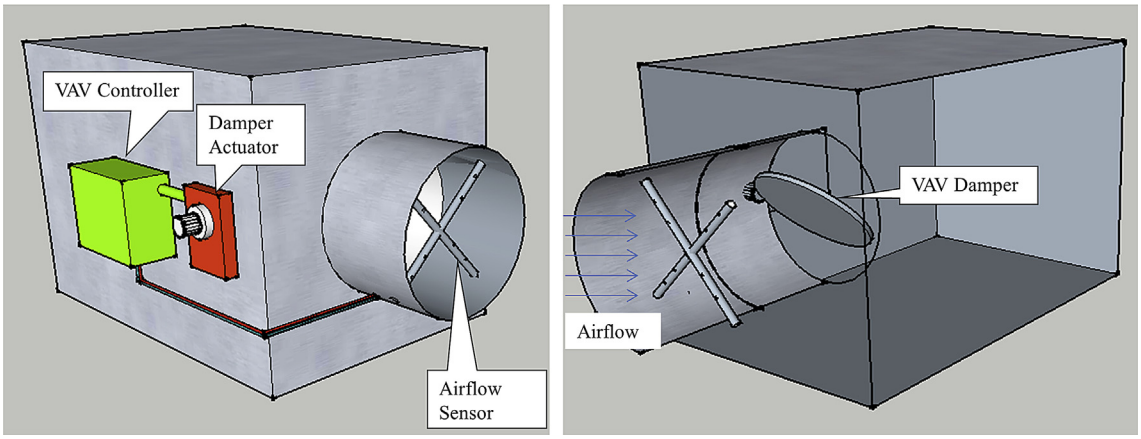


**Fig. 1.** VAV terminal unit configuration.

could cause inaccuracy of VAV airflow measurement. One of the most important factors was the non-ideal inlet condition, such as an elbow and kinked duct, as shown in Fig. 2; a kinked inlet condition could cause VAV airflow reading error up to 45% [3]. On-site balancing is regarded as a solution to correct the VAV airflow measurement error, but it only works when an accurate reference airflow measurement is available, which may be difficult to achieve practically in the field. Two methods are commonly used in the field to measure reference airflow rates: the velocity traverse method (upstream of VAV box) and the flow hood method (downstream of VAV box). For a satisfactory performance of the velocity traverse method, ASHRAE standard [5] recommends that the measuring point be located at least 7.5 duct diameters downstream and 3 diameters upstream from a flow disturbance. In practice, this requirement is rarely met in the field, resulting in non-ideal inlet conditions as the norm [4]. The flow hood method measures the airflow coming out of the diffusers. It is not affected by non-ideal inlet conditions upstream of the VAV box, but it does not account for the leakage of the duct connecting the VAV box to diffusers. This leakage is included in the airflow reading taken by the VAV flow sensor and cannot be ignored. The field test of ASHRAE RP-1353 shows that the leakage between the VAV box and the diffusers can be in excess of 100 cfm, which is often more than 20% of the minimum airflow rate for typical 8 in. VAV boxes. Therefore, it is very difficult to correct the non-ideal inlet condition effect by on-site balancing.

### 1.2. Flow conditioner review

Non-ideal inlet conditions cause large errors in VAV airflow measurements because a non-ideal inlet condition causes irregular air velocity profiles. In typical VAV boxes, flow is inferred from pressure readings, and the limited pressure sensing ports on the VAV airflow sensor may not well represent the airflow profile and thus result in measurement errors. The hypothesis of this work is that if the velocity profile were regulated before going through the VAV airflow sensor, then the measurement accuracy could be improved. Therefore, the impact of a flow conditioner on VAV measurement accuracy is systematically studied here to examine the potential improvement it can afford under non-ideal inlet conditions.

A flow conditioner is a device that regulates the flow profile and removes the swirl, cross-flow, and asymmetry in fluid flow. Thus, with a flow conditioner upstream of a VAV box, flow with a more fully developed velocity profile should encounter the VAV pressure sensors and ensure higher measurement accuracy. The use of flow conditioners is a common approach to improve the accuracy of flow measurements and has been well studied; however, no study was found in the open literature that examined the application of a flow conditioner for an HVAC airflow measurement, particularly on a VAV airflow sensor.

Flow conditioner studies focus often on improving the perturbation-removing effect on a specific flow meter, such as an orifice meter, and reducing the pressure drop across the flow conditioner. For example, Laws [6], Erdal [7], Spearman et al. [8], and Manshoor et al. [9] studied perforated plates (Fig. 3(a)–(c)) and evaluated impacts of the parameters of overall porosity, the grading of porosity along the radius, the wetted perimeter, the perforation distribution, and the number and size of holes in the plate. The graded porosity was very important for developing a velocity profile as fully as possible, and the blocking area on the plate was related to the conditioner pressure drop and turbulent kinetic energy. Laws and Quazzane [10,11] studied the Zanker flow conditioner, which is a combination of a graded perforated plate and a honeycomb section, and the thickness of the plate played an important role and the honeycomb became removable if the plate was thick enough. Ouazzane, Benhadj [12] and Laws [13] designed a Vaned Laws plate flow conditioner consisting of a graded perforated plate with upstream vanes (Fig. 3(d)), and it well removed the swirl and produced a fully developed flow field. Frattolillo and Massarotti [14] compared the performance and pressure drop of different types of flow conditioners, and concluded that the hybrid flow conditioners like Zanker flow conditioner and Vaned Laws plate could generate fully developed velocity profiles in a shorter distance downstream but had higher pressure drops compared to perforated plates only.

A common method to evaluate the performance of a flow conditioner is to examine the velocity profile downstream of it. The velocity profiles at different distances downstream, such as 5D (i.e., 5 $\times$ duct diameter, D), 10D, 15D, etc., are compared to those of an ideal duct condition (i.e., long enough straight ducts for flow to fully develop). A high performance flow conditioner should fully develop the velocity profile and remove flow swirl and asymmetry in as short a distance as possible [6–8].

Other than the ability to regulate the velocity flow profile, the pressure drop across the conditioner is also an important factor when evaluating flow conditioner. An increased pressure resistance in the flow consumes more fan energy, so a flow conditioner should have the lowest pressure drop possible [15]. To express the pressure drop independent of velocity, it is common to define the pressure loss coefficient as the pressure drop across the flow conditioner over the velocity pressure, shown in Equation (1):

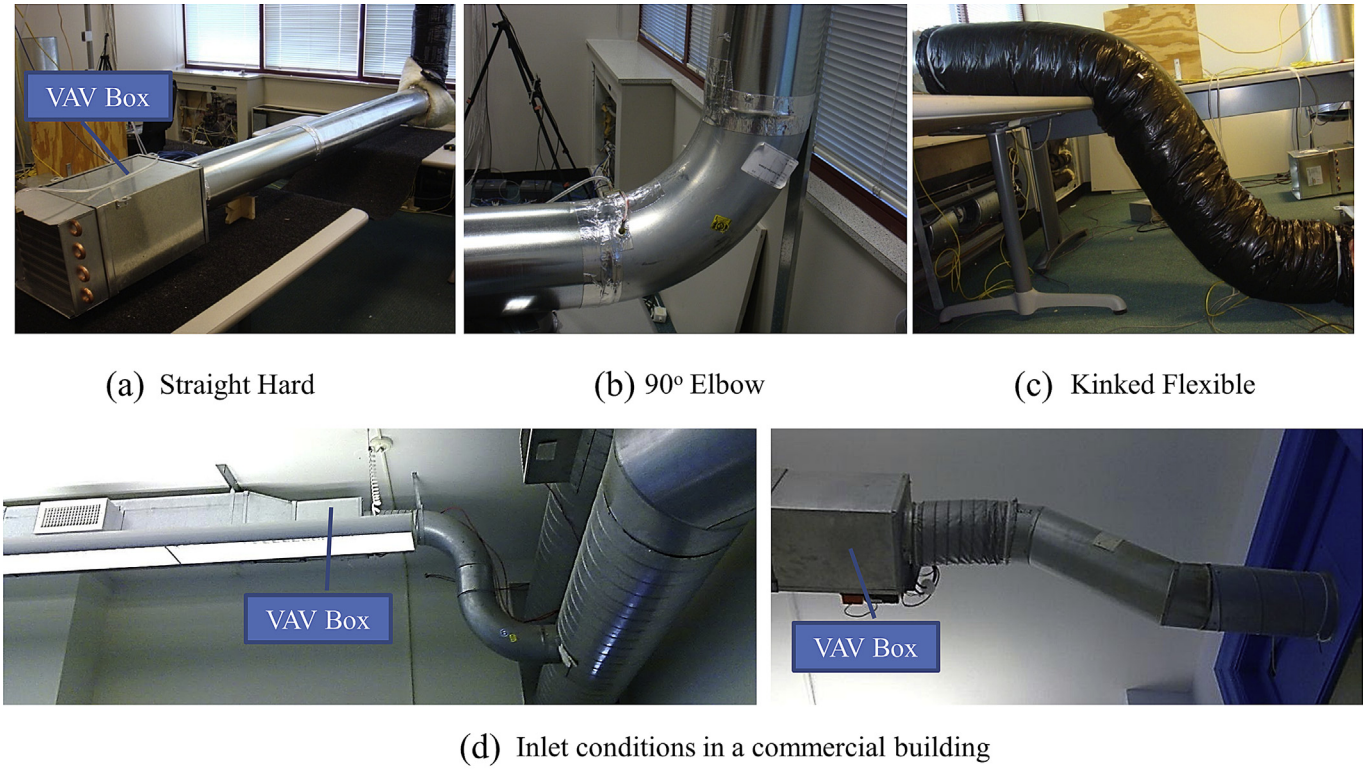


**Fig. 2.** VAV inlet conditions.

$$PL = \frac{\Delta P}{\left(\frac{1}{2}\rho u^2\right)} \quad (1)$$

where, $PL$ is pressure loss coefficient, dimensionless; $\Delta P$ is the pressure drop caused by the flow conditioner, Pa; $u$ is the average velocity in the duct, m/s; $\rho$ is the density of the air, kg/m$^3$.

The smaller the $PL$ value, the better the conditioner is in terms of pressure loss. Therefore, flow conditioner design is an optimization process between the sensor measurement accuracy improvement and the pressure drop/fan energy use.

Both experimental testing and computational fluid dynamic (CFD) modeling were used in previous studies on flow conditioners

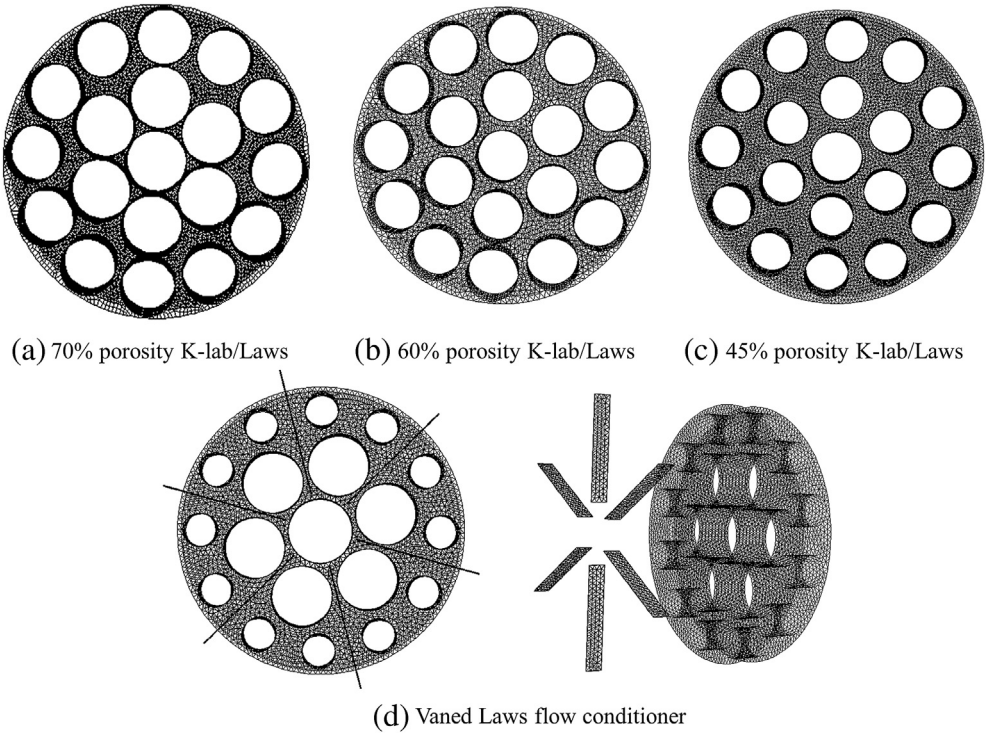


**Fig. 3.** Modeled flow conditioners with mesh on the surface.

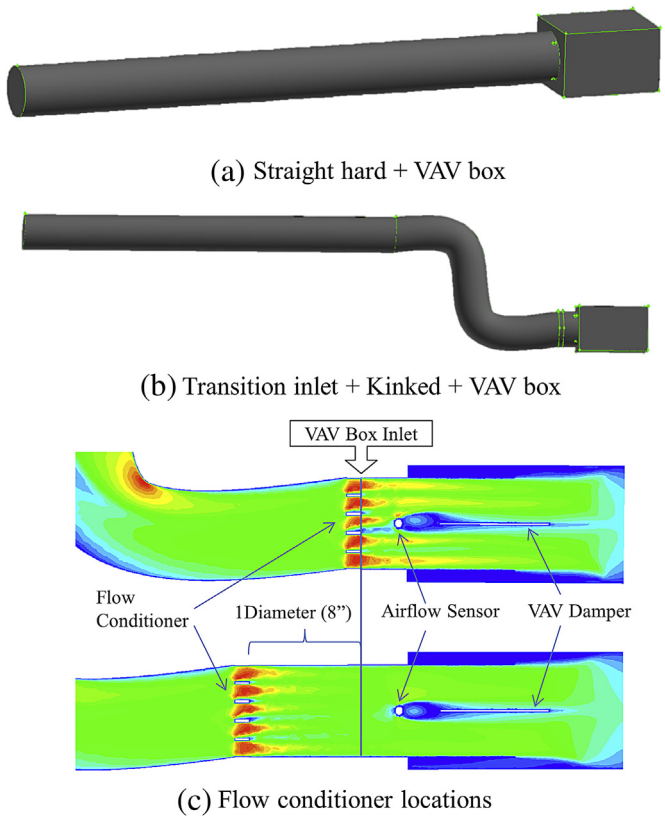


**Fig. 4.** Simulated CFD virtual test bed.

[7,16,17]. In this work, the feasibility of designing a flow conditioner to increase the airflow measurement accuracy for a VAV box was explored. To do so, a variety of flow conditioners were evaluated using computational fluid dynamics (CFD) modeling, and then an optimized prototype was fabricated and tested in a laboratory environment.

## 2. Flow conditioner design and CFD modeling

CFD modeling was first used to evaluate different flow conditioners and their abilities to improve VAV airflow measurement accuracy. A CFD virtual test bed was developed as the calculation domain, and then four flow conditioners were simulated and compared.

### 2.1. CFD technical settings

#### 2.1.1. Calculation domain

The virtual test bed is shown in Fig. 4(a)–(c) and included an inlet condition, an 8 in. VAV box, a flow conditioner, and a straight duct prior to the VAV inlet. A two-axis airflow sensor (shown in Fig. 5(a)) was modeled for the VAV flow sensor. Only one type of VAV airflow sensor was modeled because the ASHRAE RP-1353 project [3,4] revealed that different VAV airflow sensors performed similarly. Two inlet conditions representing an ideal and a non-ideal inlet condition were modeled, namely straight and kinked duct conditions, respectively. Based on previous CFD studies on elbows and flexible ducts regarding pressure drop issues [18,19], a 10D (7 ft) long straight duct was added prior to the inlet condition to ensure a velocity profile similar to that of a real straight duct before the VAV box inlet. For each inlet condition, three VAV damper positions were modeled: 100%, 35%, and 25% open.

#### 2.1.2. Mesh scheme

An unstructured triangle–tetrahedral grid was generated for this CFD study. It produces finer grids on intersections and boundaries to capture important viscous effects, and has more freedom on varying mesh density to meet the needs of the calculation domain [20,21], which is necessary for the complex geometries of the VAV sensor, damper, and flow conditioner. The grids were first generated on all surfaces with boundary layers, including the surfaces of the sensor, damper, flow conditioner, cylindrical ducts and rectangular box. Then the interior space of the calculation domain was meshed. An unstructured triangle–tetrahedral grid was applied to both face mesh and volume mesh. Finer grid sizes were generated in the near-surface regions.

#### 2.1.3. Grid sensitivity test

The initial grid density was set at 73,000 nodes/ft$^3$ as a starting point based on the literature [18]. To ensure the grid density was large enough, a grid sensitivity test was performed. The basic procedure was to increase and decrease grid density by 50% and compare the results to those of the initial density. A grid sensitivity test was performed each time the geometry of the model varied (damper position, inlet condition, etc.). Velocity profiles generated by different grid densities were compared at the following locations: box inlet, in between sensor and damper, and after damper. The simulation at the higher grid density resulted in a difference of less than 1% at the VAV box inlet and less than 3% at the other locations, relative to the initial density, so it was concluded that the initial grid density of 73,000 nodes/ft$^3$ was sufficient for this study.

#### 2.1.4. Turbulence model selection and validation

Three turbulence models, namely, Reynolds Stress Model (RSM), Standard $\kappa$–$\varepsilon$ Model, and Re-Normalization Group (RNG) $\kappa$–$\varepsilon$ Model were considered in this study. Using the RSM, the residual of continuity did not converge at low flows (50 and 100 cfm) and low damper positions (25% and 35% open). The RNG $\kappa$–$\varepsilon$ model was superior to the Standard $\kappa$–$\varepsilon$ Model, as noted by Refs. [22,23], and converged successfully and required fewer iterations, especially at low flows (50 and 100 cfm) and low damper positions (25% and 35% open).

To validate the CFD model, the velocity profiles predicted by the RNG $\kappa$–$\varepsilon$ model were compared to ASHRAE RP-1353 laboratory test data, for which velocity profiles were measured at the inlet of a VAV box. The percent differences between the CFD-simulated velocity and tested velocity were within ±5%.

### 2.2. Flow conditioner design

Different flow conditioner designs based on literature recommendations were evaluated within the CFD calculation domain, including two classes of flow conditioners, namely K-Lab/Laws flow conditioners and hybrid flow conditioners.

#### 2.2.1. K-Lab/Laws flow conditioners

According to Ref. [14], K-Lab/Laws flow conditioners (shown in Fig. 3(a)–(c)) have pressure loss coefficients as low as 0.3, remove swirl effects and asymmetries of velocity profiles efficiently, and are easy to manufacture. The porosity, defined as the ratio of perforated area to the total area of the plate, is a key factor determining the performance and pressure drop of a K-Lab/Laws flow conditioner [7], so we modeled porosities of 70%, 60%, and 45%. Based on Refs. [6,7], the thickness of the flow conditioner was fixed at 1/8D (1 in. for 8 in. duct). For each porosity case, four airflow rates of 50, 100, 200, and 700 cfm were simulated at the 100% open damper position first, and the flow conditioner with best performance was then also evaluated at the 35% and 25% open damper

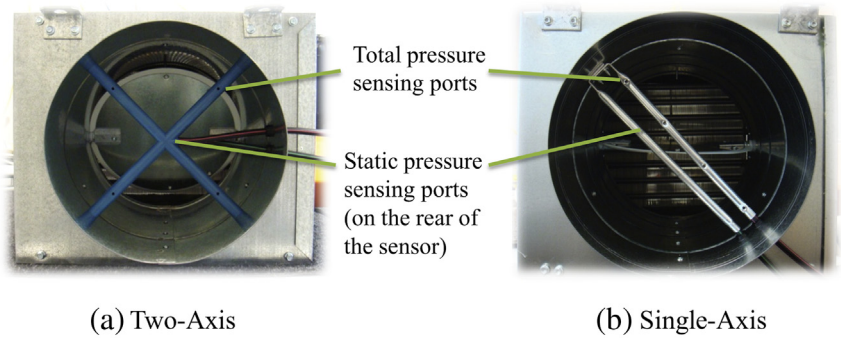


**Fig. 5.** VAV airflow sensors.

positions. The perforation distribution on K-Lab/Laws flow conditioner was set at the common 1:6:12 [6,7], meaning that one central hole was surrounded by six holes in an inner concentric row and 12 holes in an outer concentric row so that 19 holes with identical diameters were equally distributed (Fig. 3). The actual arrangement is not that important to the results and was not varied in our optimization, as Erdal [7] showed that different perforation arrangements with the same porosity resulted in similar performances in regulating the velocity profile.

Two locations of the flow conditioner relative to the VAV box inlet were simulated, shown in Fig. 4(c). One was at the VAV box inlet, which was ~0.34D upstream from the VAV flow sensor face, and the other was 1D upstream from the VAV box inlet. For those VAV boxes that are tested in this paper, the distance from the VAV box inlet to the VAV flow sensor is about 0.34D. Considering that during a field installation, the VAV box inlet is the most convenient location to place the flow conditioner, 0.34D was chosen as one of the two test locations. Another location, 1D (a typical distance suggested by the literature) upstream to the VAV box inlet was also chosen, to understand how location might affect the flow conditioner's performance. Since the purpose of the flow conditioner is to reduce the need of long straight duct, no other locations were tested.

### 2.2.2. Hybrid flow conditioners

The hybrid flow conditioner was also considered because previous studies have shown that hybrid devices better remove swirl and asymmetry and generate more fully developed velocity profiles in less distance downstream than K-Lab/Laws flow conditioner [10,12]. The drawbacks were higher pressure loss (0.8–1) and higher difficulty to manufacturer. Being time consuming in geometry generation and CFD simulation, the hybrid flow conditioner was given less emphasis in this study, and only one type, the Vaned Laws flow conditioner, shown in Fig. 3(d), was examined. The Vaned Laws plate has already been optimized in the literature [12], and as such, the vane with a length of 1 in. was placed upstream of a perforated plate with 50% porosity and there was a 4 in. air gap between the plate and the vane. In addition, the vanes were placed such that no flow channels in the plate were blocked. Other than evaluating only a fixed porosity, the same testing procedure was used for the Vaned Laws plate as the K-Lab/Laws flow conditioners.

### 2.2.3. Virtual VAV airflow reading error

In practice, a pressure-based VAV airflow sensor (shown in Fig. 5) infers the airflow velocity pressure and converts it to a VAV airflow rate. Specifically, the VAV airflow sensor measures the total pressure at the sensing ports located on the front of the airflow probe facing the airflow, while static pressure is measured at the sensing ports located on the rear side of the airflow sensor. The difference between these two is the amplified velocity pressure (VAV differential pressure) [24]. A VAV airflow sensor may have multiple total pressure sensing ports and/or multiple static pressure sensing ports, and their total effect is averaged for the final flow inference. Using the following equation, the measured VAV differential pressure is converted to the VAV airflow rate:

$$Q_{VAV} = K\sqrt{\Delta P_{VAV}} \tag{2}$$

where, $Q_{VAV}$ is the VAV volumetric airflow (cfm); $\Delta P_{VAV}$ is the VAV differential pressure (in. of water); and $K$ is the conversion factor provided by the VAV manufacturer (cfm/in. of water $^{0.5}$). Usually, the $K$ factor is determined by the manufacturer from measurements of differential pressure versus airflow rate under idealized ductwork conditions. To evaluate the VAV airflow measurement percent error, $\%Error_{VAV}$, the following equation is defined:

$$\%Error_{VAV} = (Q_{VAV} - Q_{REF})/Q_{REF} \times 100 \tag{3}$$

where, $Q_{REF}$ is the reference airflow rate (cfm), which is measured by high-accuracy airflow station and regarded as the "true flow".

To evaluate the flow conditioner performance in CFD simulation, a virtual VAV airflow reading error was calculated based on the real pressure measuring mechanism above, with the procedure described as follows:

(1) Before running a CFD simulation, the inlet airflow rate was specified as a boundary condition and was regarded as the virtual reference airflow rate, $Q_{REF\_CFD}$, that the virtual VAV airflow rate measurement was compared against.
(2) From the simulation result, the total pressure and static pressure at any point within the calculation domain were known, so the total pressure, $P_{T\_CFD}$, and the static pressure, $P_{S\_CFD}$, at all pressure sensing ports could be determined. The virtual VAV differential pressure, $\Delta P_{CFD}$, was calculated as:

$$\Delta P_{CFD} = P_{T\_CFD} - P_{S\_CFD} \tag{4}$$

where $P_{T\_CFD}$ is an average of the total pressures at all total pressure sensing ports shown in Fig. 5, and $P_{S\_CFD}$ is an average of the static pressures at all static pressure sensing ports.

(3) Using the virtual test bed with a straight hard inlet condition, cases were simulated with inlet airflow rates and the $\Delta P_{CFD}$ for each case was calculated. Knowing $Q_{REF\_CFD}$, a virtual $K$ factor, $K_{CFD}$, was determined by the following relation:

$$K_{CFD} = Q_{REF\_CFD}/\sqrt{\Delta P_{CFD}} \tag{5}$$

The calculated virtual $K$ factors under different damper positions and airflow rates are listed in Table 1. All cases in Table are with straight hard inlet condition.

**Table 1**
Virtual $K$ factors under different damper positions and airflow rates in CFD simulation.

| Simulated airflow, cfm | Virtual $K$ factor, cfm/in. of water $^{0.5}$ | | |
|---|---|---|---|
| | 100% open damper | 35% open damper | 25% open damper |
| 100 | 1052.78 | 1101.31 | 1080.71 |
| 200 | 1076.45 | 1143.46 | 1152.27 |
| 700 | 1072.40 | N/A | N/A |

This $K_{CFD}$ was then used in the virtual test bed with kinked flexible inlet condition and flow conditioner design cases to determine the virtual VAV airflow rate, given as:

$$Q_{VAV\_CFD} = K_{CFD}\sqrt{\Delta P_{CFD}} \quad (6)$$

(4) Finally, a virtual VAV airflow reading error was calculated as:

$$\%Error_{CFD} = (Q_{VAV\_CFD} - Q_{REF\_CFD})/Q_{REF\_CFD} \times 100 \quad (7)$$

An optimized flow conditioner would be expected to keep this error to below ±5%.

### 2.3. Results and discussion

#### 2.3.1. Virtual VAV airflow reading errors and velocity profiles

Fig. 6 shows the virtual VAV airflow reading errors of different flow conditioner designs at the 200 cfm simulated airflow rate, and similar results were obtained with the 100 and 700 cfm tests. For the 100% open damper position, the error for the kinked duct inlet condition with no flow conditioner was about 7%. With the flow conditioners immediately before the VAV box inlet, the VAV airflow reading error was even larger, up to about 34%. However, the errors became much smaller when the flow conditioners were 1D upstream before the VAV box inlet. At this position, the K-Lab/Laws flow conditioners yielded a virtual VAV airflow reading error of less than ±5%. Among the 1D downstream position cases, 60%-porosity yielded the smallest absolute error of about −1%.

The velocity profiles at the virtual VAV flow sensor position for the different cases are plotted in Fig. 7, and the diamond dots refer to the velocity along the horizontal center line while the square dots represent the velocity along the vertical center line. The velocity is 0 fpm at the center of each velocity profile because of the blocked area at the center of the VAV sensor. The velocity profiles after the kinked duct inlet were distorted when compared to that after a straight duct inlet. Also, the velocity profiles when the flow conditioner was immediately upstream of the box inlet showed large disturbances at the sensor because the sensor position was too close to the flow conditioner. The velocity profiles for a conditioner 1D upstream from the VAV box are better developed and are similar to those after a straight duct.

Simulation results using the Vaned plate indicate that this hybrid conditioner does not yield a better result than the K-Lab/Laws flow conditioner as the literature indicated, potentially due to the perforation distribution of the plate. As shown in Fig. 3(d), there are larger perforations in the center of the conditioner and smaller ones in the outer row, which results in a concentrated airflow mass along the central line. This concentration resulted in more negative pressure on the rear side of the VAV flow sensor where the VAV static pressure is sensed, and therefore, the virtual airflow reading error increased.

For the 100% open damper position testing condition, the 60%-porosity plate performed better than the 70%-porosity and 45%-porosity plate, as well as the Vaned plate. Two damper position cases, 35% and 25% open, were then simulated to verify the performance of the 60%-porosity plate at these lower damper positions. Consistent with the 100% open damper case, the 60%-porosity plate placed immediately before the VAV box inlet yielded larger errors than that with the kinked flexible inlet condition only. However, the error reduced to less than 3% when the plate was placed 1D downstream of the inlet.

#### 2.3.2. Pressure drop of modeled flow conditioners

Table 2 lists the pressure drops and pressure loss coefficients of the simulated flow conditioners. All numbers are the average results from all of the different inlet conditions and flow conditioner locations, as these factors did not influence the pressure drop meaningfully. The pressure loss coefficient calculated using Equation (1) ranges from 0.27 to 0.4 for the K-Lab/Laws flow conditioners, which is consistent with the literature [14]. The Vaned plate yielded higher pressure loss coefficients than those of a K-Lab/Laws plate, although the pressure drops from a Vaned plate were not necessarily larger than those from a K-Lab/Laws plate.

### 2.4. Summary from the CFD modeling study

The simulation results showed that the best design, in terms of reducing VAV airflow error and pressure loss, was a 60%-porosity K-Lab/Law plate, so this flow conditioner was selected as the prototype to be evaluated in the laboratory test. The simulation results also showed that the effect of the flow conditioner on the velocity profile at the sensing point was highly dependent on its location relative to the VAV box inlet (i.e., immediately before or 1D upstream). Also, it is worth noting explicitly that the calculation of the VAV differential pressure in the CFD setting was simplified and averaged discrete points directly. This may result in a difference from actual VAV airflow measurement. Section 3.3 compares the CFD modeling with the laboratory testing.

## 3. Flow conditioner laboratory test

### 3.1. Experimental design

Based on the CFD studies, an 8 in. diameter prototype of the best-performing VAV flow conditioner, which was the 60%-porosity K-Lab/Law plate, was designed and then fabricated at the Drexel University Machine Shop. The prototype and its dimensions are shown in Fig. 8. The prototype was manufactured for an 8 in. VAV box because of its widespread use.

#### 3.1.1. Test bed setup

A laboratory test rig (schematic in Fig. 9) was developed to test the impact of the flow conditioner on the VAV box measurement accuracy. A blower with speed control was located upstream of all ductwork to provide the desired airflow, followed by a flow box serving as the connection between the blower outlet and the 2 ft. long straight, round 8 in. diameter ductwork, followed by the inlet conditions tested in this study, and then the VAV box. A pressure probe on the straight duct measured the supply air static pressure.

Three inlet conditions were tested: straight hard, 90° elbow, and kinked flexible. The straight hard duct was a 5 ft. long with 8 in. diameter straight duct, so with the 2 ft. upstream duct, a 7 ft. long straight hard inlet condition was created. This distance is long enough to remove the disturbances caused by the blower and flow box (>7.5D downstream) [5]. The kinked duct was positioned as a Ω-shape because pre-tests revealed the shape was expected to yield

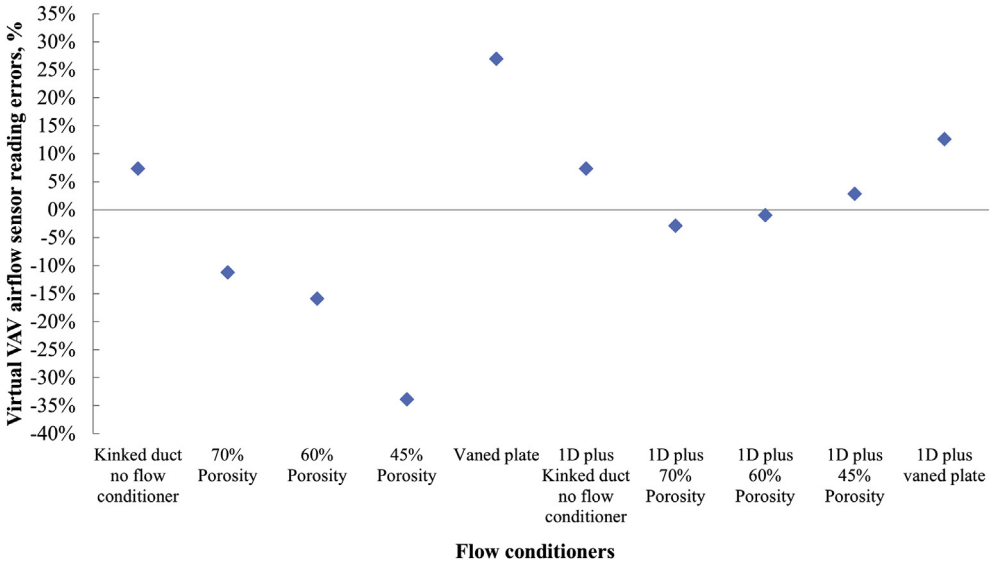


**Fig. 6.** Virtual VAV airflow reading errors under different flow conditioner settings at 200 cfm set point and 100% open damper position.

the largest VAV airflow reading errors. Each inlet condition was tested with and without the flow conditioner, and the flow conditioner was placed at the two positions tested in the CFD modeling, i.e., immediately before the VAV box inlet and 1D (8 in.) upstream of the VAV box inlet. The VAV box inlet was ~0.34D from the VAV flow sensor, as it was with the CFD modeling. When testing the flow conditioner 1D upstream of the VAV box, one extra pressure sensor was used to measure the pressure drop across the flow conditioner. This sensor could not be used when the flow conditioner was right before the VAV box inlet due to limited space.

The VAV damper position was controlled by an actuator with an ON/OFF motor switch. During a fixed supply air pressure test, the damper position was adjusted manually to achieve desired supply air pressure and airflow rate, and an angle scale was marked behind the actuator to indicate the damper position. The VAV box outlet was connected to a flow hood box, which also had its static pressure measured and was followed by a reference flow station. Close attention was paid to ensure the air tightness of the entire ductwork especially the part from the VAV box inlet to the end of reference flow station. Bubble tests were performed to examine the leakage along all joints.

A Duct Blaster (Energy Conservatory) [25] served as the reference airflow station. Similar to a powered flow hood, the Duct Blaster measures airflow by maintaining a zero differential pressure

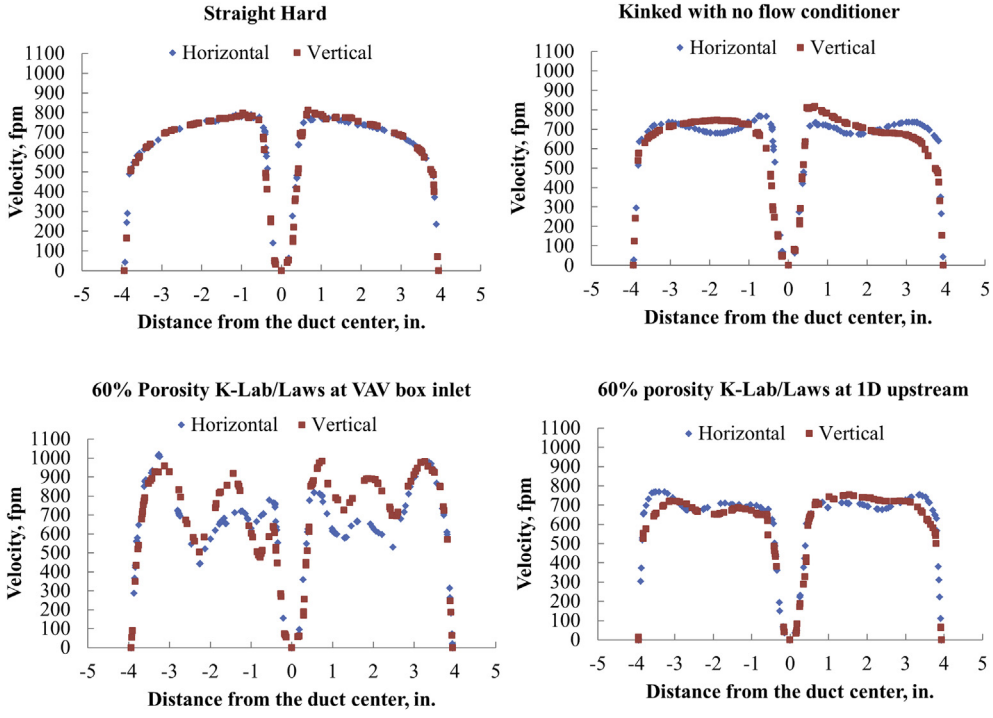


**Fig. 7.** Simulated velocity profiles at VAV airflow sensor (200 cfm set point).

**Table 2**
Pressure drop and pressure loss coefficients of CFD-simulated flow conditioners.

| | | K-Lab/Laws | | | Vaned plate |
|---|---|---|---|---|---|
| | | 70% porosity | 60% porosity | 45% porosity | |
| Pressure drop at different airflow, in. of water | 50 cfm | 0.0017 | 0.0027 | 0.0053 | 0.0037 |
| | 100 cfm | 0.0035 | 0.0056 | 0.012 | 0.011 |
| | 200 cfm | 0.016 | 0.025 | 0.055 | 0.048 |
| | 700 cfm | 0.18 | 0.28 | 0.63 | 0.53 |
| Pressure loss coefficient (calculated using Equation (1)) | | 0.27 | 0.33 | 0.40 | 0.42 |

between the flow hood box and the ambient environment and reading the airflow rate generated by a variable speed, built-in fan. The manufacturer rated maximum uncertainty of the reference flow station was ±3%, and the total uncertainty of each airflow rate was calculated considering the uncertainties from the airflow sensor, the pressure transducer, and the air density effect. The calculated flow uncertainties are listed in Table 3.

The sampling rate was 1 Hz for all recorded data. In each case, 10 minutes of data after the conditions were at steady state were used for analysis, where steady state was defined as when the reference flow station reached the desired flow rate and the flow hood box pressure was maintained at zero. In addition, the supply air pressure was maintained at 0.5 in. of water.

#### 3.1.2. Test cases

Three inlet conditions were examined in this study, each of which was tested with and without the flow conditioner positioned at two locations. Two VAV boxes with different airflow sensing mechanisms were tested, namely a single-axis sensor and a two-axis sensor. The single-axis box was the exact box tested in the ASHRAE RP-1353 project [3,4], and the two-axis VAV box was a used VAV box provided by Drexel. Both fixed damper and fixed pressure tests were performed. During the fixed damper test, the damper position was fixed at 100% open to examine the impact of the flow conditioner without any damper interference. Under this test, airflow rates including 100, 200, 300 cfm, and a max flow rate, were tested by varying supply air pressure, where the max flow rate was the maximum flow rate generated by the blower and was ~600 cfm for the straight hard and elbow inlet conditions and ~400 cfm for the kinked inlet condition. For comparison, 400 cfm was also tested for straight hard and elbow inlet conditions. During the fixed supply air pressure tests, 0.5 in. of water duct static pressure was maintained, and the VAV damper positions were varied to provide the desired airflow rates of 100, 200, and 300 cfm.

Testing procedures were similar to those used during the laboratory test described in ASHRAE RP-1353 project [3,4]. Several cases were randomly selected to be repeated. The test results were evaluated by the VAV airflow reading $\%Error_{VAV}$ defined as in Equation (3), which also uses Equation (2). For all cases, the VAV airflow readings of $Q_{VAV}$ were calculated using the default $K$ factors provided by the VAV box manufacturers, and it was $K = 927$ cfm/in. of water $^{0.5}$ for the single-axis box and $K = 890$ cfm/in. of water $^{0.5}$ for the two-axis box. The reference airflow reading, $Q_{REF}$, was that provided by the reference airflow station.

### 3.2. Results and analysis

#### 3.2.1. Straight hard inlet

Fig. 10(a) shows the test results for the straight hard inlet condition at the 100% open damper position. For the single-axis sensor, the VAV airflow reading errors with the straight hard inlet condition were around 3% at all airflow set points, consistent with those from the laboratory test in ASHRAE RP-1353 project, which indicated that using the default $K$ factor would yield satisfactory airflow measurement accuracy. Interestingly, with the flow conditioner at the VAV box inlet, the VAV airflow reading errors increased to 8–13%, potentially because the flow conditioner resulted in uneven velocity profiles immediately upstream of it. However, with the 1D straight duct between the flow conditioner and the VAV box inlet, the VAV airflow reading errors decreased back to 3%, similar to those for just the straight hard inlet condition. Results from the fixed pressure test (summarized in Fig. 11(a)) are similar to those from the fixed damper test, indicating that VAV damper positions and supply air pressures do not affect the test results within the range of our experimental conditions.

For the two-axis sensor, the VAV airflow reading errors with the straight inlet condition ranged between −4 and −8%. Similar to the single-axis sensor, the flow conditioner immediately upstream of the VAV airflow sensor caused larger airflow reading errors of between −5 and −9%, but again, when the flow conditioner was placed 1D upstream of the VAV sensor, the errors reduced back to less than −5% at low flows and less than −8% at high flows. The differences were even smaller in the fixed pressure test, which are in Fig. 11(a), though the fixed pressure test results were overall similar to those from the fixed damper test.

#### 3.2.2. Kinked inlet condition

The test results of the single-axis box for kinked inlet conditions are shown in Fig. 10(b) for the fixed damper tests and in Fig. 11(b) for the fixed pressure tests. The VAV airflow reading errors were about 40% under kinked inlet conditions for nearly all tested airflow set points. With the flow conditioner between the kinked inlet and the VAV box, the airflow reading errors decreased to 1–4%, similar to results for the straight hard inlet condition. With a 1D straight

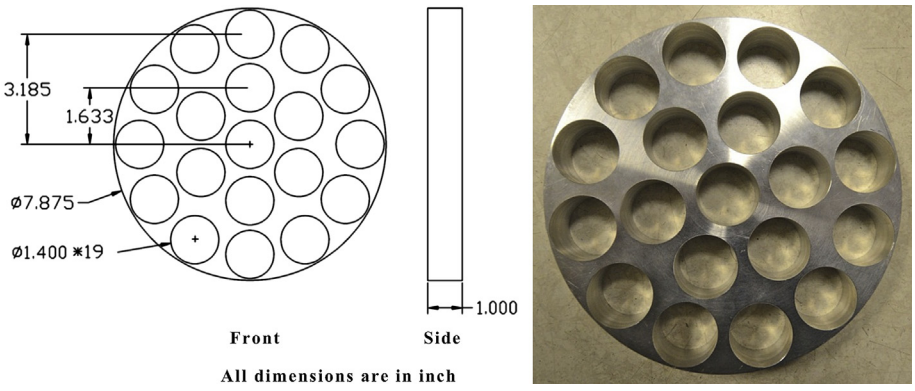


**Fig. 8.** The prototype of the VAV flow conditioner.

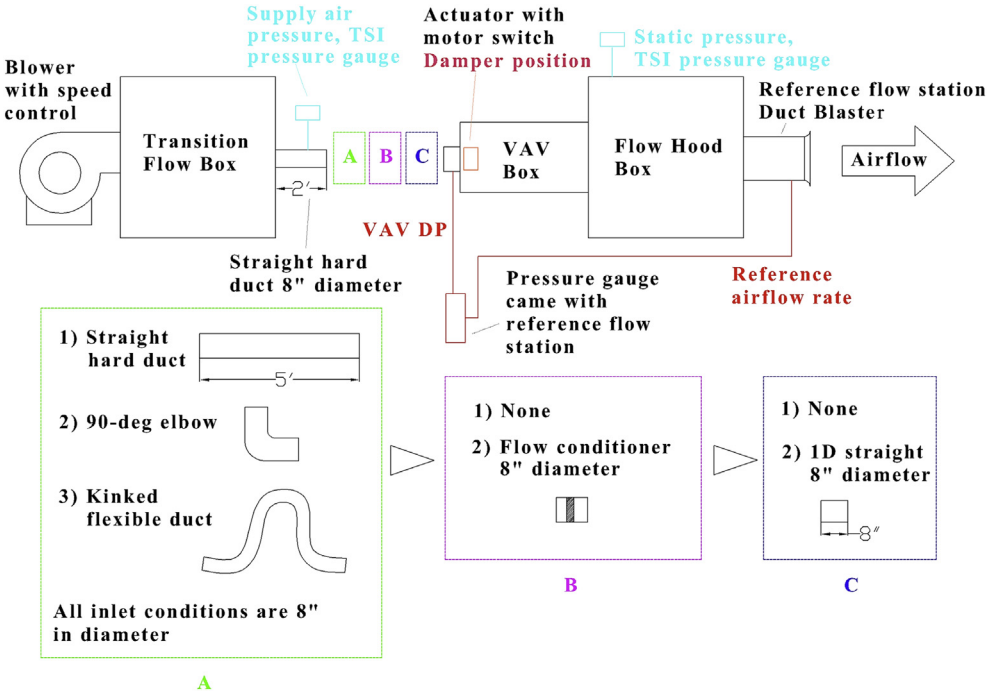


**Fig. 9.** VAV flow conditioner laboratory test setup.

duct (no flow conditioner) between the kinked inlet and the VAV box, the airflow reading errors were about −5%, implying that the 1D straight duct addition did not reduce airflow reading errors caused by kinked duct as effectively with only the flow conditioner. In conflict with the CFD predictions, the flow conditioner plus 1D straight duct configuration did not further reduce the airflow reading errors, which were 2–7%. Results from the fixed damper tests and the fixed pressure tests were similar.

The test results of the two-axis box under kinked inlet conditions are also shown in Fig. 10(b) for the fixed damper tests and in Fig. 11(b) for the fixed pressure tests. The VAV airflow reading errors were about 13% under kinked inlet conditions for nearly all tested airflow set points, and with the flow conditioner between the kinked inlet and the VAV box, the airflow reading errors decreased to ±2%, which was even smaller than those under the straight hard inlet condition. With the 1D straight duct (no flow conditioner) between the kinked inlet and the VAV box, the airflow reading errors were about −9 to −13%, so the addition of a 1D straight duct did not reduce airflow reading errors caused by the kinked duct for the two-axis airflow sensor. The flow conditioner plus 1D straight duct configuration did not further reduce the airflow reading errors, which were 1–4%, below those for just the flow conditioner. Results from the fixed damper tests and the fixed pressure tests were similar.

### 3.2.3. Elbow inlet condition

Fig. 10(c) shows the fixed damper test results for the single-axis box with the 90° elbow inlet condition. The VAV airflow reading errors for this condition were 10–21%, and the flow conditioner alone reduced this error to less than 5%. Unlike the case with the kinked inlet, the 1D straight duct after the elbow (no flow conditioner) increased the VAV airflow reading error to 10–13% (except for 5% at 100 cfm). Moreover, the flow conditioner plus 1D straight duct configuration yielded even larger VAV airflow reading errors of 10–15%. Additional tests were performed to explore this phenomenon, which are discussed in Section 3.2.4. Fig. 11(c) shows the fixed pressure test result, and with the damper variation, the above conclusions were still valid but the absolute values of the error terms decreased by about 2%, when compared with those from the fixed damper tests.

The 90° elbow test results of the two-axis box displayed in Fig. 10(c) and Fig. 11(c) indicate that the elbow inlet condition did not result in more than 6% VAV airflow reading error for the two-axis box that was tested, which was even smaller than for the straight hard duct inlet condition, so testing the combination of elbow and 1D straight duct was not performed. The flow conditioner was quite effective in reducing the errors for this elbow inlet, which were the smallest among those from all inlet conditions.

### 3.2.4. Additional velocity pressure test

The above laboratory test results demonstrate that the flow conditioner is more effective at improving tested VAV airflow sensor accuracy when it is installed immediately before the VAV box inlet rather than at 1D upstream of the box inlet. However, the CFD simulation results indicated that the latter location should yield a more evenly distributed velocity profile, leading one to expect that the latter location would yield a better VAV airflow measurement accuracy, which was not observed in our experiments.

To explore this conflict, a Pitot tube was used to measure the velocity pressures across the duct cross section at a point very close to the VAV sensor for the single-axis VAV box. As shown in Fig. 12(a), velocity pressures were measured along four traverses: horizontal, along the sensor, vertical, and across the sensor. Along each traverse, velocity pressures were measured at seven locations (with only four sensing ports along the single-axis sensor), at 200 cfm of airflow with a 100% open damper position for five inlet

**Table 3**
Uncertainty of reference airflow station in the flow conditioner test setup.

| Airflow rate, cfm | 50 | 100 | 200 | 300 | 400 | 600 |
|---|---|---|---|---|---|---|
| Uncertainty, ±cfm | 1.25 | 2.54 | 5.02 | 7.52 | 10.07 | 15.20 |

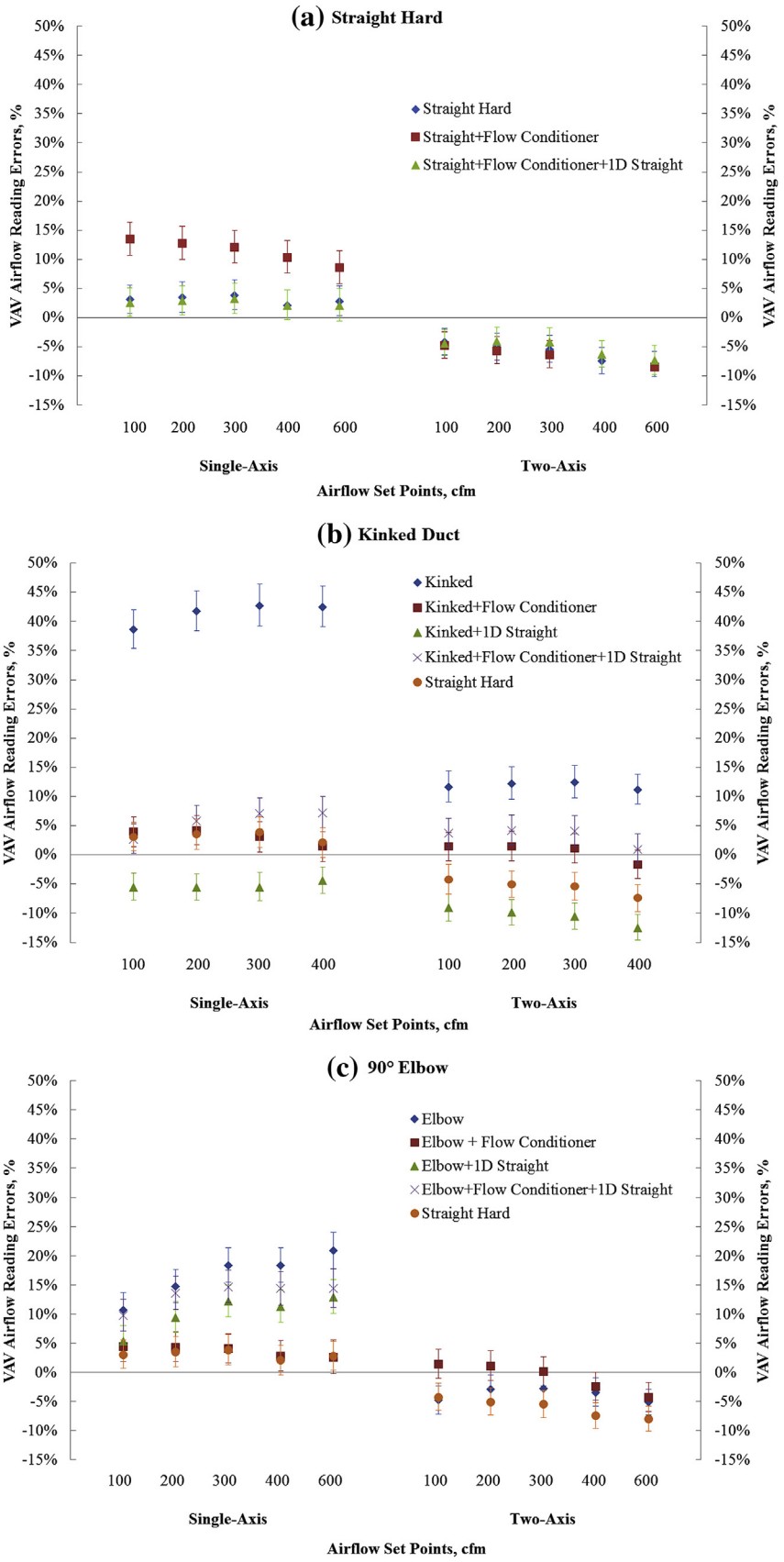


**Fig. 10.** Flow conditioner test results at 100% open damper position.

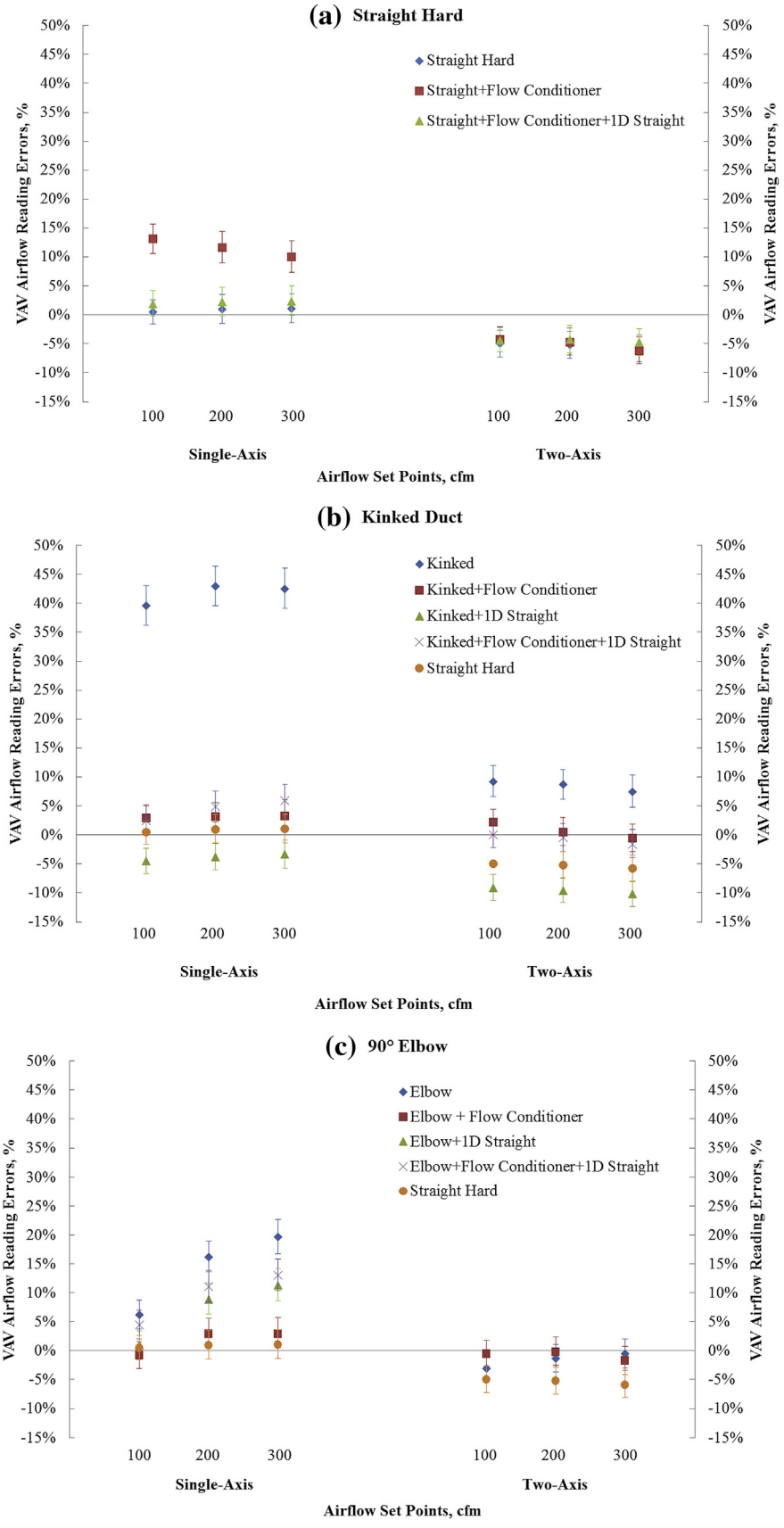


**Fig. 11.** Flow conditioner test results at 0.5 in. of water duct static pressure.

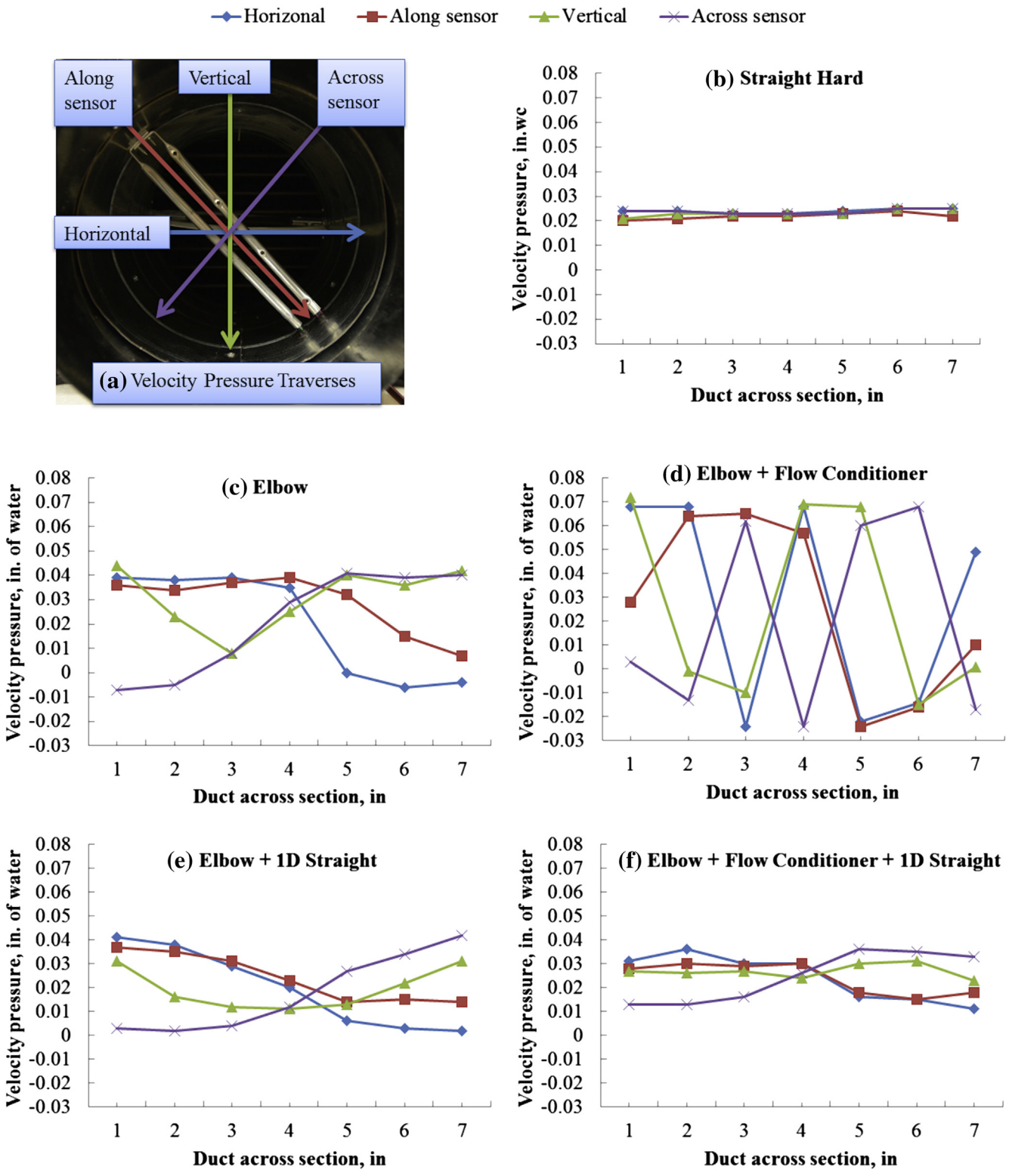


**Fig. 12.** Velocity pressures measured by Pitot tube.

condition and flow conditioner (FC) combinations: straight, elbow, elbow + FC, elbow + 1D straight duct, and elbow + 1D + FC.

The velocity profiles are very different for the five tested inlet combinations. Fig. 12(b) shows the results at straight duct inlet condition: the velocity pressures at each traverse are fairly uniform, at 0.023 in. of water. Fig. 12(c) shows the results for the elbow inlet condition. Compared to the straight duct, a larger velocity variation exists at each traverse, indicating a less uniform velocity profile. At the traverse along the VAV sensor, the velocity pressures at most of the tested locations were higher than those from the straight inlet condition, explaining why the VAV airflow was higher for the elbow inlet condition than the straight hard condition. However, rotating

the sensor would not correct this problem since the velocity pressures along other axes are also either much higher or lower than the corresponding straight duct values. As such, a two-axis VAV sensor would improve the measurement accuracy only modestly.

With a flow conditioner installed immediately upstream of the VAV box inlet, the velocity pressure variation along any axis is larger than any other inlet combinations, as shown in Fig. 12(d). However, the variations along any axis include both high positive pressure and high negative pressure, indicating even a single-axis sensor could average out the variations since it has multiple openings along the sensor. Fig. 12(e) shows the velocity pressures for the elbow + 1D straight duct inlet condition. Compared to the elbow only case, smaller variations were observed because the 1D straight duct smoothed out the velocity profile; however the measured VAV airflow reading error was still greater than that under the straight duct. As shown in Fig. 12(f), with the flow conditioner 1D upstream of the VAV box inlet the smallest variation in velocity pressures was observed among the four elbow cases, at similar magnitude to the straight duct. However, the velocity pressures were still not uniform enough to generate VAV airflow reading errors comparable to the straight duct.

Previous flow conditioner studies have made efforts on developing a uniform velocity profile at a downstream distance as short as possible. But it is shown in this study that the VAV airflow sensor could be located very close (0.34D) to the flow conditioner, where the velocity is still strongly fluctuating. At this location, the VAV airflow measurement error is close to that of a straight hard inlet condition, not because of a fully developed velocity profile, but because the typical VAV sensor could effectively average out the velocity variations. Further downstream of the flow conditioner, the velocity profile starts to develop and its fluctuation reduces, and in this case, the performance of the VAV airflow sensor relies on the development of the velocity profile. 1D downstream of the flow conditioner was not enough to reduce the airflow reading error due to a non-ideal inlet condition, but it is believed that further downstream of the flow conditioner could result in a satisfied VAV airflow measurement.

### 3.2.5. *Pressure drop of the VAV flow conditioner*

The pressure drop of the flow conditioner at each flow rate was measured with the flow conditioner at 1D upstream from the VAV box inlet, as plotted in Fig. 13. For reference, the pressure drop of the flow conditioner was compared to the pressure drop of typical VAV box reheat coils, using data obtained from a single-axis VAV box manufacturer [26]. (The pressure drop of a two-axis VAV box reheat coil is similar to a single-axis VAV box [27].) Fig. 13 illustrates that the pressure drop of the flow conditioner was approximately equivalent to the pressure drop of a typical 2-row reheat coil. The pressure loss coefficient at different airflow rates and inlet conditions ranged from 0.33 to 0.48, which were consistent with simulated results by CFD. These losses are equivalent to the pressure loss in an 8 in. straight duct ranging 29–34 ft long.

### 3.3. *Comparison of laboratory testing and CFD modeling*

Differences exist between the laboratory test results and the CFD predictions. Specifically, the CFD modeling results showed that the flow conditioner caused the smallest error (±1%) when placed 1D upstream of the VAV box inlet and that the error was larger (>10%) with the flow conditioner right before the VAV box inlet. However, the laboratory tests showed that at the location immediately before the VAV box inlet, the flow conditioner always reduced the error to ±5% for both elbow and kinked inlet conditions. At 1D upstream of the VAV box inlet, the flow conditioner also

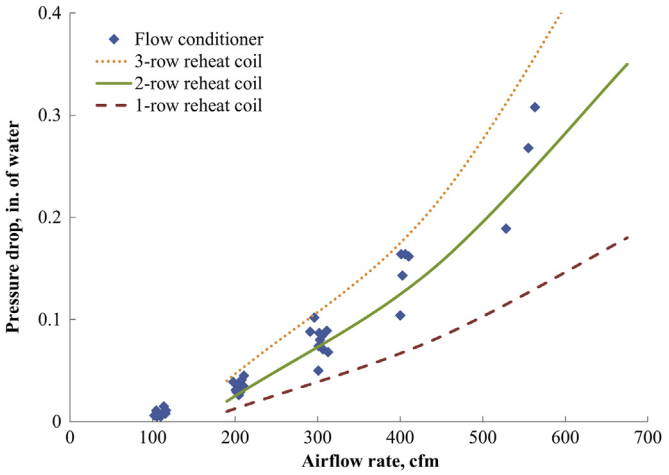


**Fig. 13.** Pressure drops of the flow conditioner prototype and typical VAV reheat coils.

reduced the reading error caused by the kinked inlet condition, but resulted in ~10% error for the elbow inlet condition. This section explores these discrepancies.

A closer look at the sensor modeling approach in the CFD test bed shows why the virtual VAV airflow sensor might result in a different reading from the actual one. Due to the complexity of modeling the micro-scale airflow inside the VAV airflow sensor, a simple solid block was modeled to represent the VAV airflow sensor in the CFD model. As stated in Section 2.3, the virtual VAV differential pressure was obtained by averaging the pressures at various surface points of the virtual VAV airflow sensor. In a real VAV sensor, however, the pressures sensed at different points are mixed and averaged inside the sensor tubes before sending the signal to a pressure transducer, potentially resulting in differences from the model approach.

An additional Pitot tube measurement was performed to explore the difference between the VAV airflow sensor measurement and the result of averaging the measured pressures of single sensing points. Fig. 14(a) displays Pitot tube measurement locations as white dots, which correspond in location to the pressure sensing port locations on the single-axis airflow sensor. The Pitot tube total pressure sensing port was faced forward to measure the total pressure and faced backward to measure the static pressure. The static pressure sensing port on the Pitot tube, normally perpendicular to the air stream, was blocked at all times during these measurements. The VAV differential pressure was obtained at each point and the average of them was compared to the VAV differential pressure reported by the VAV airflow sensor.

Fig. 14(b) displays the VAV airflow sensor measurements and the Pitot tube measurements for all inlet conditions and flow conditioner setups at a flow of 200 cfm, and clear differences exist. The largest difference is for the case with the flow conditioner between the elbow and VAV box inlet, with a difference of ~0.02 in. of water, which translates to a flow difference of ~40 cfm. The smallest is for the straight duct inlet condition, where the difference between the two measurements is ~0.003 in. of water. This comparison illuminates a possible reason why the CFD and laboratory tests yielded different results by indicating that the method of averaging the pressures measured separately (as with the virtual VAV sensor) may not represent the real VAV differential pressure measurement.

Differences in velocity profiles between the laboratory testing and the CFD modeling were not able to be assessed as a possible reason for conflicting laboratory and CFD results because velocity profiles were not measured for the same case modeled in CFD. Note

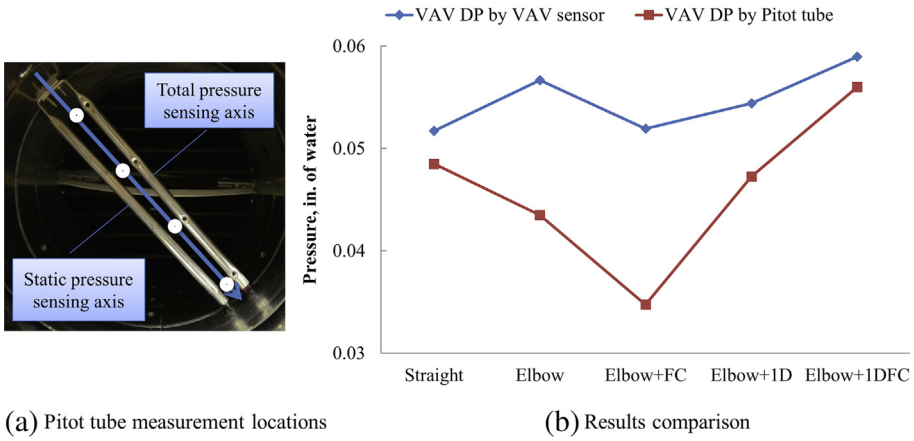


**Fig. 14.** Comparison between the VAV airflow sensor measurement and the Pitot tube measurement.

that the laboratory test was not meant to validate the CFD model but to test the performance of the prototype flow conditioner selected based on the CFD simulation under the real world conditions.

## 4. Conclusion

ASHRAE RP-1353 [3,4] showed that non-ideal inlet conditions, such as an elbow or a kinked duct, can be a major cause of large airflow measurement errors for VAV boxes at low flow conditions. This study designed a flow conditioner to cost-effectively improve VAV airflow measurement accuracy under non-ideal inlet conditions. A simulation study using a virtual test bed developed in a CFD environment was first used to optimize the design of a flow conditioner, and then a real experimental test bed was used to validate the effectiveness of the designed flow conditioner for typical 8 in. VAV boxes. Three inlet conditions, namely, straight hard, 90° elbow, and kinked flexible, as well as five supply airflow rates of 100, 200, 300, 400, and 600 cfm were tested, for both fixed supply air pressure and fixed damper position conditions with two VAV boxes with single-axis and two-axis pressure-based airflow sensors.

The laboratory tests conducted in this study on the flow conditioner prototype showed that 60%-porosity K-Lab/Laws plate reduced the VAV airflow reading errors caused by non-ideal inlet conditions such as kinked and elbow inlet conditions. With the flow conditioner installed immediately before the VAV box inlet, the VAV airflow reading error was always within ±5% for all tested inlet conditions and airflow rates for both single-axis and two-axis VAV boxes. The prototype of the flow conditioner had a pressure drop equivalent to that of a 2-row VAV reheat coil. More studies should be conducted in the future to explore other design options, such as decreasing the thickness of the plate and increasing the porosity, to further reduce the pressure drop while maintaining adequate flow conditioner performance.

## References

[1] U.S. Department of Energy. Annual energy outlook. Energy Information Administration; 2013. http://www.eia.gov/forecasts/aeo/.
[2] Klaczek W, Fleming P, Ackerman M, Fleck B. Field performance assessment of VAV control systems to determine the longevity of recommissioning. ASHRAE Trans 2005;111. Part 1.
[3] Liu R, Wen J, Zhou X, Klaassen C. Stability and accuracy of VAV box control at low flows, part 1 laboratory test setup and VAV sensor test. HVAC&R Res 2013. http://dx.doi.org/10.1080/10789669.2013.790736.
[4] Liu R, Wen J, Zhou X, Klaassen C, Regnier A. Stability and accuracy of VAV box control at low flows, part 2 controller test, system test, and field test. HVAC&R Res 2013. http://dx.doi.org/10.1080/10789669.2013.794087.
[5] ASHRAE. Measurement and instruments. ASHRAE handbook – fundamentals; 2009 [Chapter 36].
[6] Laws EM. Flow conditioning – a new development. Flow Meas Instrum 1990;1:165.
[7] Erdal A. A numerical investigation of different parameters that affect the performance of a flow conditioner. Flow Meas Instrum 1997;8(2):93–102.
[8] Spearman EP, Sattary JA, Reader-Harris MJ. Comparison of velocity and turbulence profiles downstream of perforated plateflow conditioners. Flow Meas Instrum 1996;7(3/4):181–99.
[9] Manshoor B, Nicolleau FCGA, Beck SBM. The fractal flow conditioner for orifice plate flow meters. Flow Meas Instrum 2011;22(3):208–14.
[10] Laws EM, Ouazzane A. Effect of plate depth on the performance of a Zanker flow straightener. Flow Meas Instrum 1992;3(4):257–69.
[11] Laws EM, Ouazzane AK. Further study into the effect of length on the Zanker flow conditioner. Flow Meas Instrum 1995;6(3):217–24.
[12] Ouazzane K, Benhadj R. An experimental investigation and design of flow-conditioning devices for orifice metering. Proc Inst Mech Eng Part C (J Mech Eng Sci) 2007;221(c3):281–91.
[13] Laws EM, Ouazanne AK. Compact installations for differential flowmeters. Flow Meas Instrum 1994;5(2).
[14] Frattolillo A, Massarotti N. Flow conditioners efficiency a comparison based on numerical approach. Flow Meas Instrum 2002;13(1–2):1–11.
[15] Ahmadi A. Experimental study of a new flow conditioner on disturbed flow in orifice plate metering. J Fluids Eng 2009;131(5):051104 [8 pp.].
[16] Laribi B, Abdellah Hadj A. Analysis of turbulent flow development downstream disturbers with perforated plate flow conditioner. Appl Mech Mater 2012;197:73–7.
[17] Manshoor B, Khalid A. Numerical investigation of the circle grids fractal flow conditioner for orifice plate flowmeters. Appl Mech Mater 2012;229–231:700–4.
[18] Moujaes SF, Aekula S. CFD predictions and experimental comparisons of pressure drop effects of turning vanes in 90° duct elbows. J Energy Eng 2009;135(4):119.
[19] Ugursal A, Culp C. Comparative analysis of CFD ΔP vs. measured ΔP for compressed flexible ducts. ASHRAE Trans 2006;113. Part 1.
[20] Blocken B, Carmeliet J. Validation of CFD simulations of wind-driven rain on a low-rise building facade. Original Research Article. Build Environ 2007;42(7):2530–48.
[21] Hefny MM, Ooka R. CFD analysis of pollutant dispersion around buildings: effect of cell geometry. Original Research Article. Build Environ 2009;44(8):1699–706.
[22] Chen Q, Lee K, Mazumdar S, Poussou S, Wang L, Wang M, et al. Ventilation performance prediction for buildings: model assessment. Original Research Article. Build Environ 2010;45(2):295–303.
[23] Susin RM, Lindner GA, . Mariani VC, Mendonça KC. Evaluating the influence of the width of inlet slot on the prediction of indoor airflow: comparison with experimental data. Original Research Article. Build Environ 2009;44(5):971–86.
[24] Klaczek W, Fleming P, Ackerman M, Fleck B. VAV airflow sensor response in relation to "poor" upstream duct geometry. ASHRAE Trans 2006;112. Part 1.
[25] Energy Conservatory. Minneapolis duct blaster operation manual (series B systems). The Energy Conservatory; 2009. www.energyconservatory.com.
[26] Product Data. 35E single duct terminal units for variable volume systems. Carrier Corporation; 2010. p. 17. http://www.docs.hvacpartners.com/idc/groups/public/documents/techlit/35e-6pd.pdf.
[27] Performance Data. Single/duct terminal units. Titus Corporation; 2008. p. 15. http://www.titus-hvac.com/utility/getfile2.aspx?fileid=8314.